TURBOMACHINERY & PUMP SYMPOSIA | HOUSTON, TX
SEPTEMBER 15-17, 2020
SHORT COURSES: SEPTEMBER 14, 2020

ACCELERATED TEST VALIDATION USING PRINTED POLYMER COMPONENTS

Christopher J. Guerra
Development Engineer
Siemens Energy
Olean, NY, USA

James M. Sorokes
Principal Engineer / Engineering Fellow
Siemens Energy
Olean, NY, USA

Scott P. MacWilliams
Manager, Development Testing
Siemens Energy
Olean, NY, USA

Kirk R. Lupkes
Engineering Manager, Seattle Technology Center
Siemens Energy
Seattle, WA USA

Christopher Guerra is a Development Engineer at the Olean location for Siemens Energy (formally Dresser-Rand). Christopher first joined Dresser-Rand as a Co-Op student in the Aero-Thermo Design Group for two summers. He graduated from Rochester Institute of Technology in 2013 with a Bachelor of Science and Master of Science in Mechanical Engineering. After graduation Christopher joined Dresser-Rand full-time as a Development Engineer. As a Development Engineer his responsibilities include design of testing vehicles, additive manufacturing, and instrumentation.

Scott MacWilliams is a manager of the Development Testing at the Olean location of Siemens Energy (formerly Dresser-Rand). He is a 1994 graduate of The University at Buffalo with a B.S. in Mechanical Engineering. He began his career with Dresser-Rand in 1995 as a Tooling Designer, which quickly transitioned to Rotor Center Manufacturing Engineer lasting for 9 years. Following that he became the Final Assembly Manufacturing Engineer in 2006. In 2008 Scott was promoted to General Foreman for the main Assembly and Packaging areas. In 2010 he moved to a Project Engineering role for Development Testing, responsible for execution of the assembly and testing of development projects at the Olean Operations. In 2015 Scott was promoted to the Manager of Development Testing in Olean. In this role he manages the development test technician and engineers supporting development testing as well as the overall responsibility for development testing that occurs at the Olean facility.

James M. "Jim" Sorokes is a Principal Engineer with Siemens Energy (formerly Dresser-Rand) with more than 40 years of experience in the turbomachinery industry. Jim first joined Dresser-Clark after graduating from St. Bonaventure University in 1976. He spent 28 years in the Aerodynamics Group and led the group for 20 years. His primary responsibilities during that time included the development, design, and analysis of all aerodynamic components of centrifugal compressors. In 2004, Jim was named Manager of Development Engineering and, in 2005, was promoted to Principal Engineer, responsible for various projects related to compressor development and testing. He is also heavily involved in mentoring and training in the field of aerodynamic design, analysis and testing. Jim is a member of ASME and the ASME Turbomachinery Committee. He has authored or co-authored more than 50 technical papers and has instructed seminars and tutorials at Texas A&M and Dresser-Rand. He currently holds several U.S. patents and has other patents pending. He was elected an ASME Fellow in 2008 and was also selected as a Dresser-Rand Engineering Fellow in 2015. He was given a Lifetime Achievement award by Hydrocarbon Processing magazine in 2019 in recognition of his contributions to the turbomachinery industry.

Kirk Lupkes is the Engineering Manager responsible for technical and management oversight of the Siemens Energy Seattle Technology Center team. He is a 1995 honors program graduate of Washington State University with a B.S. in Mechanical Engineering and a minor in Materials Science. He also received an M.S. in Mechanical Engineering from the University of Washington in 1997. He provides program management and technical oversight on various product development efforts including playing a leadership role on next generation aerodynamic initiatives. He joined Dresser-Rand in 2014 and has worked in combustion and turbomachinery technology development for more than 20 years.

ABSTRACT

This paper describes efforts undertaken to increase the use of non-metallic components in research and development as well as component/stage validation testing. The switch to non-metallic or polymer components was driven by the need to decrease the cycle time and cost for such testing and to reduce the "time to market" for new products or components. The paper traces the chronology of polymer use from individual stationary components to rotating components to builds in which nearly the entire aerodynamic flow path is built using non-metallic materials. Test results for a rig build using polymer components are compared to results obtained using conventional metals parts. Finally, results are provided for a recent test build in which all except one component were made via 3-D printing.

INTRODUCTION

Full and sub-scale testing of centrifugal impellers and/or complete stages is commonly used to validate the aerodynamic performance of modified or new designs prior to offering products commercially. While such rig tests are invaluable for design validation and gathering the performance data required to improve prediction accuracy, the cost and schedule impact can be prohibitive. For example, it can take eight weeks or more to fabricate a centrifugal impeller from metal (i.e., aluminum or steel). Likewise, stationary components such as return channels, vaned diffusers and/or volutes can take equal or longer times to procure depending on their geometric complexity. As a result, it can take two to three months to acquire the components for a rig test after all engineering drawings are completed. It then takes several more weeks to assemble and instrument the components, install them in the rig, connect the instrumentation to the data acquisition system, and run the test. Further, if the design fails to meet the performance objectives, the cycle time to procure replacement parts causes further delays in releasing the new designs for sale to clients. Therefore, developing methods to reduce the cycle time for validation testing is of interest not only the original equipment manufacturer (OEM) but also to the end user, who benefits from the improved performance provided by the new components, stages or products; i.e., the faster the products are released to market, the sooner the end user can reap the benefits they provide.

This paper describes a development program focused on increasing the use of non-metallic components in stage validation testing. Please note that this is not a novel concept. From the earliest days of centrifugal compressor development, test rigs made use of non-metallic parts (i.e., plastic, wood, resins, etc.). Components were constructed using conventional techniques such as milling and turning… or in the case of wooden parts, via common woodworking techniques. Use of such components reduced the cost and schedule required to fabricate components for experimental rig testing.

The advent of 3-D printing or additive manufacturing provided researchers with new means to quickly prototype parts. It has long been recognized that 3-D printed polymer components can help designers and manufacturers visualize new components and identify potential construction issues. Additive manufacturing has also radically enhanced the ability to make very complex parts, i.e., parts that are nearly impossible to build as a single piece with other manufacturing processes, such as a sphere with a single piece outer shell but hollow in the middle or a single-piece turbine blade with embedded cooling passages. With advances in printable materials, the strength and durability increased to the point where it became practical to use printed components in test vehicles operating at load. The initial focus was on stationary components such as inlet guides, return channels and volutes as these components are subject to fewer and lower dynamic force than rotating elements. A wide range of polymer materials were found that could stand up to the pressure forces imposed on stationary components. These early investigations into the techniques and materials used for the non-rotating parts uncovered several factors that would be of greater concern for rotating elements. These factors, such as anisotropic material strength, will be described in the sections on *Material Properties* that follow.

STATIONARY COMPONENTS

As noted, the non-metallic materials were initially considered for the stationary test rig components due to the lower stresses and/or forces on those components. After assessing the pressure loads and stresses on the various stationary components via commonly used analytical methods, (i.e., hand calculations, FEA), decisions were made to target inlet guides, return channels, and discharge volutes (see Figures 1 and 2). Vaned diffusers were not considered due to concerns related to the dynamic pressure forces on the leading edges immediately downstream of the impeller. There was also some uncertainty about the ability to accurately print the vane leading edge shapes.

The size limitations of the available printers also caused many components to be built in segments with said segments either being glued, rail fit, dove-tailed or bolted together. As an example, the discharge volute shown in Figure 2 was printed in multiple segments that included rail fits that allowed the segments to be assembled together. Further, in an effort to increase the print speed and reduce material costs, some parts were printed with internal webbing (see Figure 3) as opposed to being printed solid (Schmitt & Wong). This, of course, reduced the rigidity of the components, so care was taken not to use this approach for any component that might be considered "highly stressed" or subjected to high pressure loads. Experience would ultimately prove that taking the extra time and using the extra material to print solid components would save time, money and disassembly / assembly costs in the long run.

Figure 1 – Polymer inlet guide vanes at left and return channel vanes at right

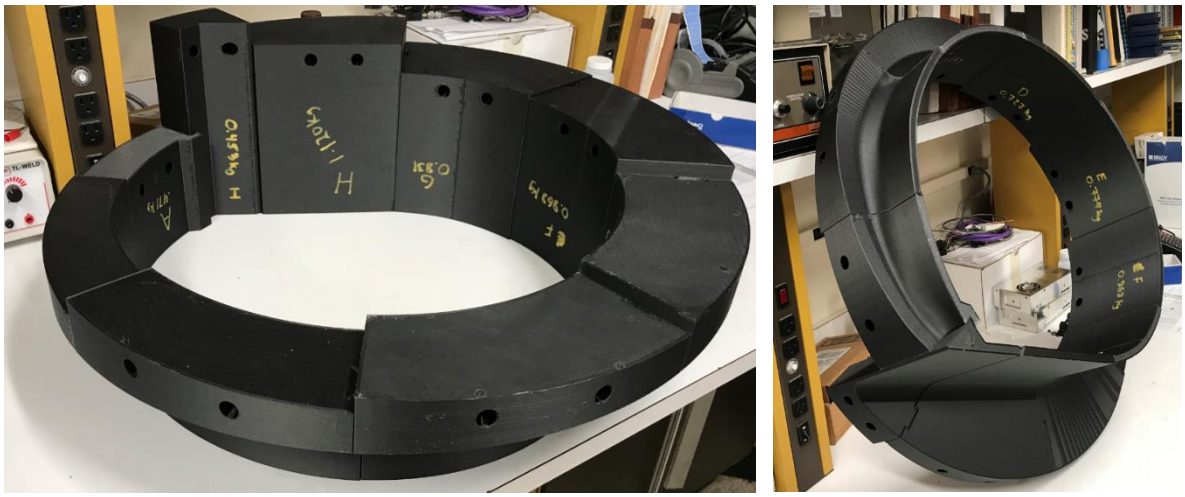

Figure 2 – Polymer Volute Assembled as Segments

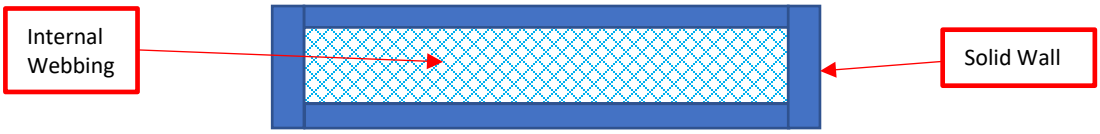

Figure 3 – Schematic Showing Internal Webbing

Methods to Augment Material Strength

As suggested in the previous sentence, some "issues" were encountered with the components built with internal webbing. In early testing, some such stationary components deflected more than expected and/or fractured when subjected to aerodynamic loads (i.e., pressure, high gas velocities). In response, three corrective measures were implemented: printing solid pieces, including additional ribbing external to the flow path, and adding metal support structures within the component. As an example of the latter, in a more recent test program, to minimize the potential for deflections of the return channel bulb, the polymer vaned return channel section and the polymer "skin" that formed the diffuser hub wall were mounted on a re-useable aluminum ring (see Figure 4). This allowed the vanes or the diffuser to be modified while using the same aluminum support piece, thus eliminating the time and cost to make the aluminum piece. There have been no further component issues related to aerodynamic load since implementing these corrective measures.

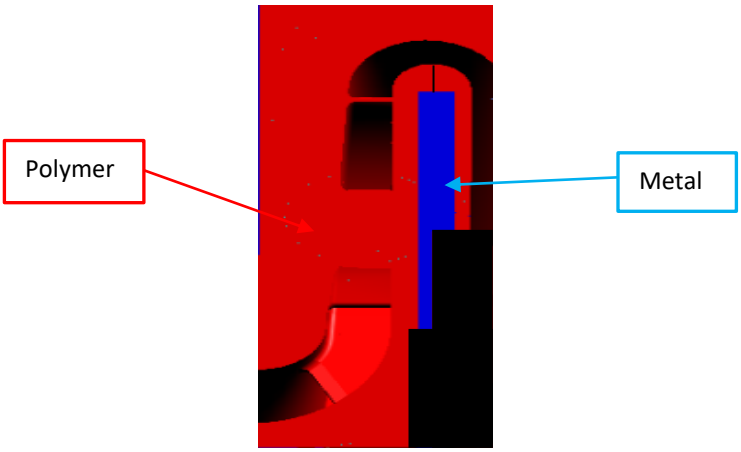

Figure 4 – Polymer return channel with metal support piece

POLYMER IMPELLERS

Having established methodologies for using printed stationary components, attention turned to determining the feasibility of using polymers or other non-metallic materials to build test rig impellers. Given the success printing dimensionally accurate stationary components, there was high confidence that a dimensionally accurate non-metallic impeller could be printed. However, many questions remained unanswered, such as:

1. Will printed impellers be strong enough to operate at the speeds required for rig testing without fracturing / failing?
2. Even if the impeller did not fracture / fail, will the geometric deformation make the data gathered useless?
3. What non-metallic or polymer materials and printing techniques can be used to minimize the above concerns?
4. Will the test gas have any detrimental effects on the material properties?
5. Are there steps that could be taken to minimize the likelihood of failure or excessive deformation?
6. Will an aerodynamic flow path comprised of polymer components provide the same performance as one constructed of conventional metals?
7. Will the tests be repeatable? That is, will permanent deformation occur during the first test that will cause subsequent use of the parts to provide different results?

Therefore, a study was undertaken to determine the answers to these and more.

IMPELLER SPIN TESTING

Initial efforts were focused on determining the mechanical strength of the various non-metallic or polymer materials. A two-fold approach was chosen for this investigation. The first step was to conduct finite element analyses (FEA) on the candidate impellers using the polymer material properties to determine if the non-metallic impeller would survive at the rotational speeds necessary for aerodynamic testing. Assuming a viable material could be found, the second step would be to conduct destructive testing in an impeller spin pit to confirm the analytical results.

Candidate Materials / Printing Techniques

There are a wide variety of materials and techniques that could be used to print impellers. Further, the industry is on a steep portion of the technology development curve with regard to materials and printing techniques. It is not the intent of this paper to summarize all of the materials or additive manufacturing methods that could be used. Numerous publications are available on these topics (Wong & Hernandez, 2012).

It must be noted that a decision was made early in the investigation to make use of third-party suppliers to make the impellers used in this test program. This decision was driven by several considerations but key among them were the cost of the printers and the desire to take advantage of the "tribal knowledge" developed by the suppliers regarding the materials and printing schemes. Printers can cost as much as $500,000 and each has limits in the materials and print schemes they can use. Further, many suppliers are in business to print parts, so it seemed prudent to take advantage of their installed equipment and expertise in building the impellers for this investigation.

Material Properties

As expected, the different materials provided a wide range of material properties. However, the printing technique provided the greater challenge from a strength perspective. To illustrate, consider the schematics shown in Figure 5. In the printing approach chosen, the material is deposited in straight lines in the "X" direction as shown in Figure 5A. An adjacent line or "bead" of material is deposited by

moving the print head in the "Y" direction. This process is repeated until an "X-Y plane" of material has been deposited. At that point, the next "X-Y plane" of material is printed on top of the first plane, i.e., at a higher "Z" dimension as shown in Figure 5B. This process is repeated until the full component is complete.

The approach described leads to anisotropic material properties, i.e., non-uniform strength depending on the direction being considered. Because the molten material is deposited continually in the "X" direction, the embedded fibers are well-distributed, providing maximum strength in the "X" direction. However, the strength is not as high in the "Y" or "Z" directions because the fibers are not well-distributed into the previously printed adjacent "beads" or lines of material. Therefore, when assessing the strength or robustness of a printed polymer impeller, one must consider these anisotropic or non-uniform material properties. It is almost certain that the impeller will deform more the "Y" direction than in the "X" direction, resulting in a slightly elliptical outside diameter.

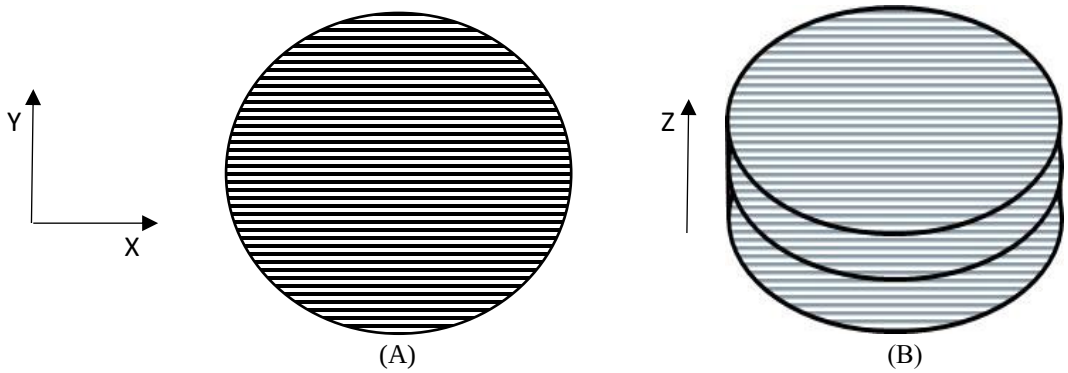

Figure 5 – Illustration of One Possible Printing Pattern

FEA Assessment

To gain insight into the extent of the deformations that might occur and to quantify the stress levels that will occur in the impeller, finite element analyses were completed on the selected impeller geometry (for example: Kim & Oh, 2008, Wohlers, 2011, Killi & Morrison, 2016). Through internal testing and working with the material manufacture, an anisotropic material data set was created and used in finite element analyses. Initial FEA showed that the impeller would survive to 13,500 rpm at room temperature with a maximum deformation of 0.032" (0.81mm). This is slightly under the target speed of 13,800 rpm. After design iterations to the non-flow path areas of the impeller, the maximum speed increased to 14,665 rpm with a maximum deformation of 0.038" (0.97mm).

Given the orientation in which the impeller was printed, the lower strength in the "Z" direction was not an issue because the main forces are from centrifugal loading. The difference in the strength between the "X" and "Y" direction did show some "ovaling" of the impeller while spinning. There was also some deformation between blades at the impeller exit as shown in Figure 6 below. The waveform at the bottom of the left image shows the deformation of around 0.03" (0.76mm) between the blades, i.e., the minor cycle, while the major cycle in the waveform is indicative of the "ovaling" of approximately 0.06" (1.52mm) at the impeller outside diameter caused by the "X" versus "Y" strength. The differences in the various diameters between the "X" (minimum deflection) and "Y" direction (maximum deflection) were considered minor but the effect of this will be quantified during the aerodynamic testing. For reference, the aluminum impeller was predicted to have no "ovaling" and no measurable deformation between blades at the test speeds.

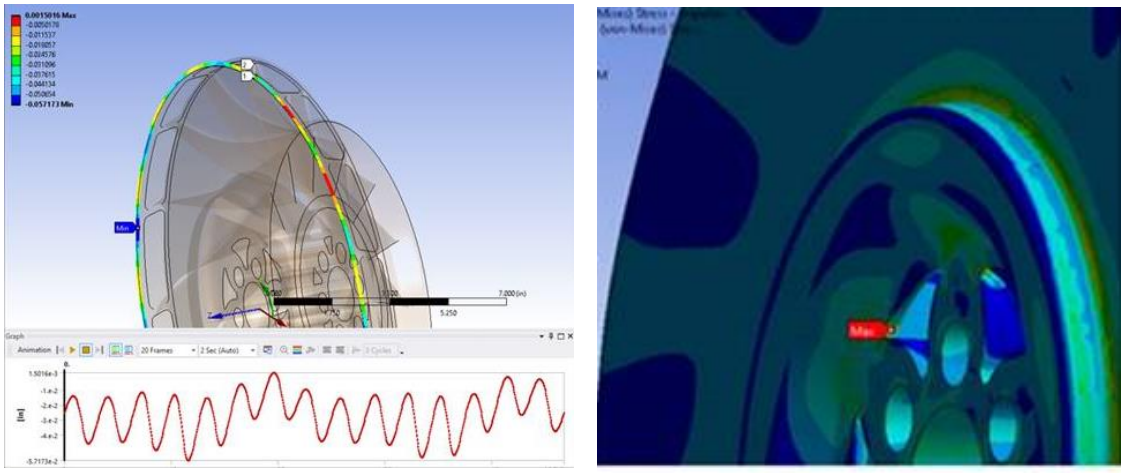

Figure 6 – FEA results showing predicted deformations of polymer impeller

Spin Testing Results

To confirm that an impeller would survive an aerodynamic test in the rig, a series of impellers were manufactured using different materials and spun in the overspeed pit until failure. The impellers included assorted changes in the disk geometry, i.e., with and without cavities for weight reduction, etc. The overspeed testing took place in a vacuum chamber at room temperature. This allowed the impeller to experience only centrifugal loading. As can be seen in Figure 7, some materials were not capable of withstanding the stresses at overspeed. When the impellers failed, it was catastrophic and only the impeller hub remained intact. The remainder of the impeller shattered due to impact against the walls of the overspeed pit (see center photograph in Figure 7). Due to the nature of the failure, the initial point, etc. could be defined.

Figure 7 – Impeller after destructive testing

After selecting the best available material for the application, additional impellers were constructed and subjected to the spin testing. The first impeller (design iteration 1) was expected to fail around 13,500 rpm based on FEA simulations using the anisotropic material properties. The impeller survived until 18,500 rpm before the quill shaft of the overspeed pit broke dropping the impeller. The second impeller run was a duplicate of the first (design iteration 1). This impeller failed at 16,000 rpm. Both of the impellers survived to a speed higher than FEA predicted, which suggests that the material properties applied in the analytical studies were not accurate. Further work needs to be done on the material properties and the FEA set up to improve the prediction, but, for now, the model is predicting the impellers conservatively, so it was decided to go forward with the current modeling approach for this test program.

The next impeller that was overspeed tested was the version that would be installed into the aerodynamic test rig. This impeller was the final design iteration. It included a some "voids" in the impeller hub to reduce some weight and was predicted to survive to 14,500 rpm. For the aerodynamic rig, the required overspeed for the impeller is 13,800 rpm. The impeller was first balanced, and measurements were taken on the eye labyrinth sealing surface and at the impeller outer diameter. After spinning the impeller at 13,800 rpm for one minute the impeller was rebalanced and inspected. The second balance showed no change. The measurements after overspeed testing did show some small dimensional changes. The impeller was then overspeed tested again to 13,800 rpm. The geometric dimensions after this run were the same as after the first test. This showed that the impeller will yield while spinning but that the dimensions will not continue to grow as long as the speed is not increased.

INITIAL POLYMER V. METAL COMPARISON

After successful testing in the over-speed pit, the next step was to assemble a complete stage in the OEMs aerodynamic test vehicle to determine if the impeller could withstand a typical validation run. The OEM had several aluminum impellers available that had been used previously for stage validation testing. A medium flow coefficient ($\phi \approx 0.08$) was selected for the comparison and a polymer impeller was built to the same drawing dimensions. Back to back tests were then completed with the aluminum and polymer impellers, with the only component changed between the tests being the impeller.

The Test Rig

The test rig used for the comparative testing was the OEMs flexible rig (Sorokes & Welch, 1991, Sorokes & Koch, 1996, Guidotti et al, 2011, Bianchinni et al, 2015, Sorokes et al, 2017). The objective of this rig build was to compare the performance of two impellers. Therefore, a simpler arrangement consisting of a radial inlet, an inlet guide, the impellers, a vaneless diffuser, and collector / volute was sufficient. The configuration was similar to that shown in Figure 8. The rig is installed in a closed loop system, permitting testing on a variety of test gases, but primarily nitrogen, carbon dioxide and R-134A refrigerant. This is important because it permits changing the test gas and the tip speed to achieve changes in the Machine Mach Number rather than only the tip speed (as is the case with open loop air testing). The rig is driven by a 1500HP electric motor through a speed-increasing gear. The peak attainable rotor speed with the current gearset is on the order of 14,000 rpm, which is beyond the speeds necessary for this test program.

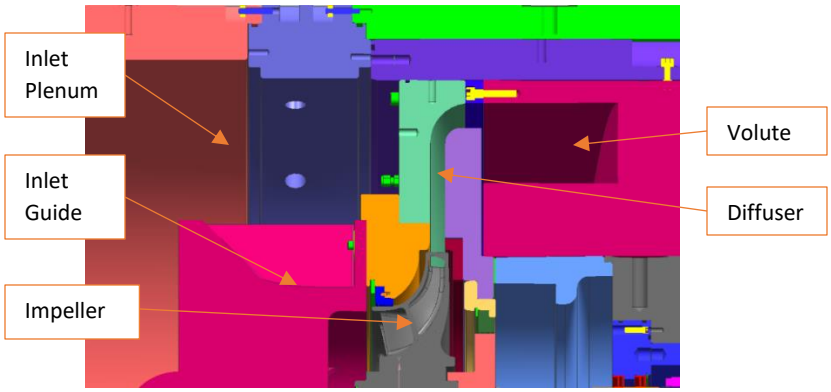

Figure 8 – Simplified test rig configuration for impeller comparison

Because of the uncertainty of the impeller's mechanical integrity and the desire to limit internal instrumentation damage, only wall static taps were installed in the primary flow path inside the rig for the initial testing. There were total temperature and total pressure probes in the inlet and discharge spool pieces. These were used to determine the overall efficiency, work input and head coefficient for the overall rig and this overall "flange-to-flange" data were used for the comparison between the metal impeller baseline and the polymer impeller. The internal static pressure taps were also used to assess the "impeller only" performance and the performance of the impeller in combination with the diffuser. Note that the same pressure and temperature probes and static pressure taps were used for both tests to remove any concerns regarding instrumentation accuracy. Likewise, the upstream and downstream stationary components were not changed between the tests. It was possible to test both impellers without changing the stationary components or the instrumentation. Finally, though impeller eye labyrinth clearance would have minimal impact on the impellers being tested, care was taken to ensure that the impeller eye labyrinth clearances were maintained at the same level between the aluminum and polymer tests. This was done by using the impeller eye deflections predicted via FEA and sizing the aluminum and polymer test labyrinths accordingly. The clearances were confirmed both before and after each run.

The impeller geometry

As noted, the selected impeller was a medium flow coefficient ($\phi \approx 0.08$) design that is part of the OEM's standard product offering. It is a full-inducer design with a ruled-surface blade as shown in Figure 9. The exit diameter of the impeller in the rig was 14.88" (378 mm) and the exit backsweep was 45°. Confidentiality requirements preclude providing further information about the impeller geometry but suffice it to say the blade angle distribution and hub and shroud profiles conformed to standard industry practices for an impeller of this flow coefficient range.

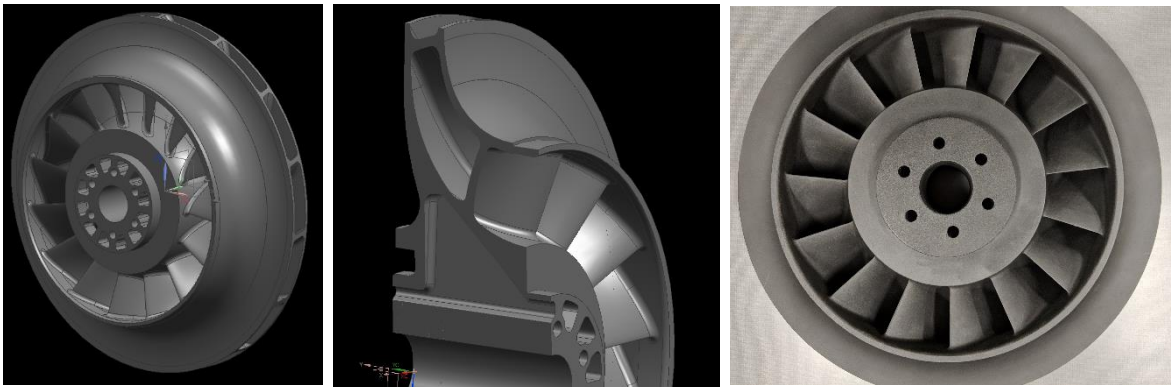

Figure 9 – Polymer Impeller – Solid model at left and center – photo of actual impeller at right

To check the relative geometry of the aluminum and polymer impellers, both were scanned using a laser system. Some discrepancies were found between the two impellers, but the deviations in critical aerodynamic parameters were less than 1% and most were in locations that would cause little or no variation in the impeller performance. The one exception was the impeller tip opening and this will be addressed in the section describing the test results. However, the surface finish of the printed polymer impeller was rougher than on the single-piece milled aluminum impeller. The aluminum impeller average surface finish was approximately 50 µin while the polymer impeller finish was closer to 250 µin. Based on 1-D models developed to account for the impact of surface finish on impeller performance, this is a large enough difference to cause a one to two-point drop in impeller efficiency for the polymer impeller. Consideration was given to applying different types of surface finish treatment including slurry finishing or other forms of polishing. These techniques were applied for subsequent impeller tests, but the initial testing was completed with the as-printed surface finishes.

The test conditions

The test plan was set up to allow for the polymer impeller to slowly step up speeds. This was done to allow for the most data to be collected in case of a failure of the impeller during testing. Table 1 outlines the test conditions.

Table 1 – Operating Conditions for Metal and Polymer Impeller Testing

Speedline	Speed, RPM	Tip Mach Number, U2/A0	Tip Speed, ft/sec (m/sec)	Gas	Inlet Temp °F (°C)	Inlet Pressure psia (bar)
1	4542	0.25	295 (89.9)	Nitrogen	100 (37.8)	60 (4.13)
2	7267	0.4	472 (143.9)	Nitrogen	100 (37.8)	60 (4.13)
3	9084	0.5	590 (179.8)	Nitrogen	100 (37.8)	60 (4.13)
4	10894	0.6	707 (215.5)	Nitrogen	100 (37.8)	60 (4.13)
5	11809	0.65	767 (233.8)	Nitrogen	100 (37.8)	60 (4.13)
6	11680	0.85	758 (231.0)	CO2	100 (37.8)	55 (3.79)
7	10164	1.2	660 (201.2)	R134a	100 (37.8)	25 (1.72)

Initial testing was done on Nitrogen to prove that the impeller would survive with aerodynamic loading at Machine Mach Numbers (U2/A0) up to 0.65. The speed was slowly increased to determine if there were differences in the performance data between the polymer and metal impeller, which had also been run over the same U2/A0 range. After completing the nitrogen runs, additional speed lines of data were gathered using carbon dioxide (CO_2 – speed line 6) and R-134A refrigerant (speed line 7) as these are the test media typically used for medium and high U2/A0 testing during stage validation. Note that these higher speed lines were completed for two different polymer impellers to compare the potential impact of additive manufacturing tolerances. The higher speed lines and heavier mole weight gases also subjected the polymer impellers to higher gas densities and pressure loads. The higher speeds with all gases provided insight into whether deformation due to impeller rotation had an effect on aerodynamic results. At the end of speed line 7, the test rig was purposefully surged for over two minutes and the polymer impeller survived this phenomenon at high gas density.

Test Results

As outlined in Table 1, multiple speed lines were run to confirm that a polymer impeller could survive aerodynamic loading and also demonstrated that polymer impeller would provide the same performance data as a metal impeller. The comparison between the metal and polymer impellers was done at speed line 4 (U2/A0 = 0.60). A plot comparing the overall flange-to-flange efficiency, work input and head coefficient for the metal and polymer impeller is provided in Figure 10. Note that the test rig inlet and discharge sections were not optimal and caused a large reduction in the overall performance. However, this does not detract from the performance comparison shown in the figure as both impellers were tested using the same inlet and discharge sections.

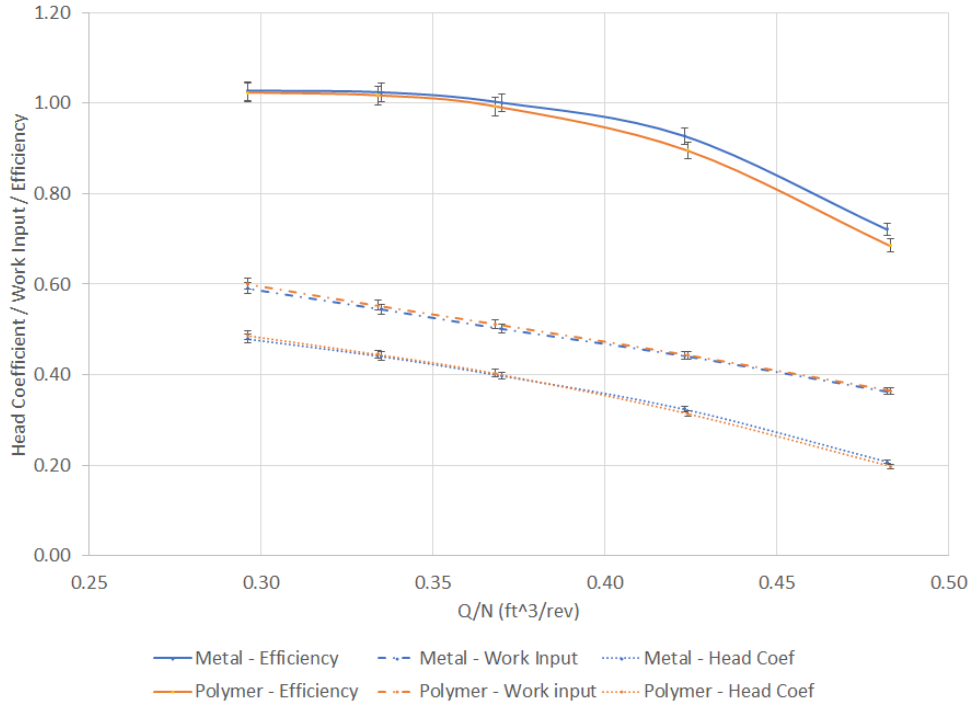

Figure 10 – Plot of Normalized Efficiency, Actual Work Input, and Actual Head Coefficient v. Flow Coefficient
[*Note: The error bands on the head coefficient and work input coefficient are the same height as the plotting symbols. Both show the location of the data point*.]

There was a good agreement between the metal and first polymer impeller. There was a small reduction in efficiency toward overload for the polymer impeller. Several factors contributed to this reduction. First, as noted, the surface finish of the polymer impeller was rougher than the metal impeller surface finish. Due to the polymer printing process, the flow path surface was similar in finish to an "as cast" part (Ra = 250 µin). Conversely, the metal impeller was single-piece machined and had a surface finish of lowers than 50 µin. As mentioned previously, the 1-D model predicted a difference as much as two points in efficiency for this variation in finish. Therefore, the test results fell within the efficiency variation predicted for the change in surface finish. Second, the laser scan results had suggested that the polymer tip opening was slightly smaller than the aluminum impeller opening. This would cause the exit velocity to be higher, resulting in higher friction losses. Third, the FEA work suggested deflections of the hub and shroud material between the blades at the impeller exit that could cause further reduction in the width and exit area. The impeller tip width reduction is also evidenced when reviewing the impeller static pressure ratio as shown in Figure 11.

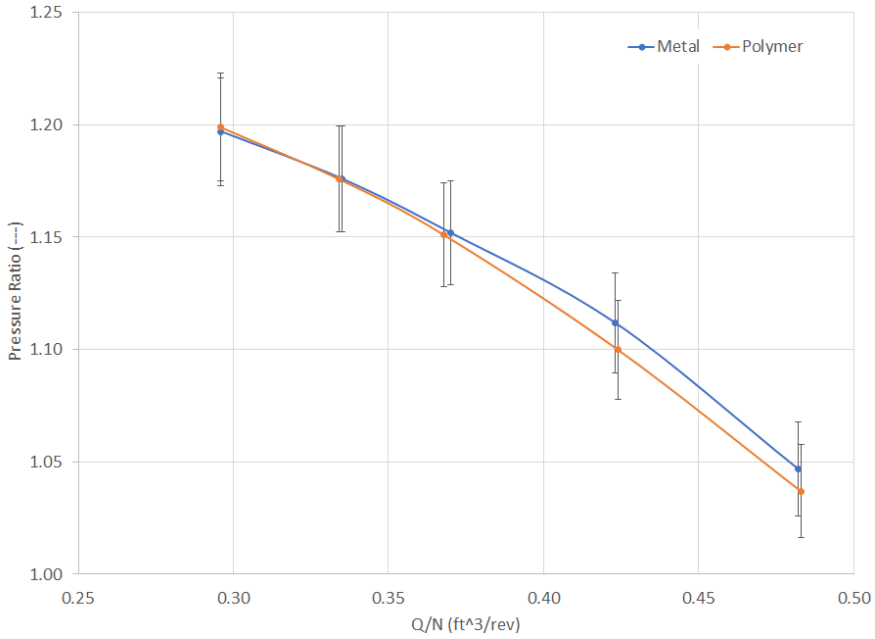

Figure 11: Normalized Impeller Static Pressure Ratio

The impeller static pressure ratio shows that, at overload, the metal impeller has a higher ratio than the polymer impeller. As the Q/N is reduced, the static pressure ratio more closely agrees between the two impellers. This suggests a smaller exit area since the higher velocity out of the impeller would result in a smaller static pressure ratio through the impeller.

The smaller exit area of the polymer impeller is not necessarily a surprise given the printing process used. Printed parts can turn out slightly undersized if the proper scaling is not done before printing. Typically, due to the heat of printing and the printing program, the part will be undersized or heavy (i.e., outside diameters are oversized, inside diameters are undersized). After some iterations to ascertain the deviations that result for a given part due the printing process, scaling factors can be used so that the part will print closer to the design dimensions. If this were done, the polymer impeller dimensions would have more closely matched the metal impeller geometry and the test result would have been even closer. Time and budget did not permit a rebuild and retest of the impeller with the necessary scaling corrections, but the lessons learned regarding the deformation of this impeller were implemented on subsequent test impellers built.

FURTHER POLYMER COMPONENT TESTING

Having proven the viability of using polymer components, a test program was initiated to validate a novel aerodynamic flow path currently under development. In this case, however, it was necessary to include all intermediate stage components including an inlet guide, an impeller, a vaneless diffuser, a return channel system and the downstream inlet guide. Therefore, the test configuration was more complex than the arrangement used for the polymer / metal impeller comparison. There were also plans to test alternative configurations for the stationary components downstream of the impeller, so a test arrangement was developed that would permit easy access to these components. Further, the of non-metallic materials was extended to include nearly all primary flow path components, including portions of the inlet section, the inlet guide vanes, the impeller, the vaneless diffuser, the return channel assembly and portions of the exit section of the rig.

A schematic representing the new build is shown in Figure 12 below. Note that this schematic does not show the actual geometry as that information is proprietary and confidential. However, the schematic does provide the reader with insight regarding the portion of the flow path that includes polymer components. As can be seen, except for a small portion of the inlet guide, the remainder of the test envelope (indicated by the dashed yellow box), including the impeller, are constructed of polymer. [Note: The term "test envelope" is

used to indicate that the primary objective of the testing is to determine the performance from the inlet of the upstream inlet guide to the exit of the downstream inlet guide. The bulk of the instrumentation will be located in that envelope.] For clarity, the metal components are colored blue in the figure while the polymer parts are colored red. Note that there are numerous metal structural members that can be re-used for subsequent builds and the case segments (different shades of blue) and heads (not shown) are also comprised of steel.

It should be noted that, as suggested above, the impellers being used in this test program were subjected to slurry finishing, which improve the surface finish to approximately 70 µin. Further, the stationary components were also polished to improve their finish to 120 µin or better.

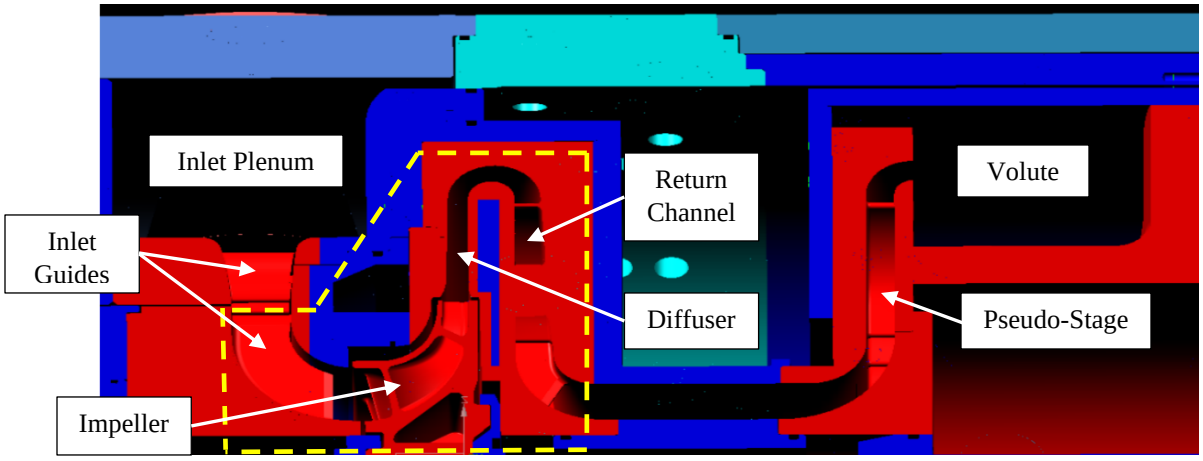

Figure 12 – Schematic showing indicating where the non-metallic (red) and metallic (various shades of blue) are used in the full-stage rig. The test envelope is enclosed in the dashed yellow box

Note that the impeller used in this testing had "voids" included in the hub section. These provided three benefits: (1) reduced use of material (lower cost); (2) reduced weight (a rotordynamic benefit), and (3) improved stress distribution.

At the time this paper was written, the first phase of the new stage development testing had been completed and the second phase was about to begin. During the first runs under phase one, some of the discharge volute segments failed. This situation was resolved by including additional polymer ribs external to the flow path. Some fatigue cracks also developed in one of the return channel walls. The original wall was printed with internal "webbing," so the replacement wall was printed solid. No polymer components experienced issues after the above changes were made. Notably, the polymer impeller has survived throughout the 40+ hours of testing conducted to date.

In this case, there was no metal equivalent tested so a comparison between metallic and non-metallic parts is not possible. However, the test data agreed very well with the CFD predictions for the candidate stage (see Figure 13). Therefore, there was sufficient confidence to proceed with the next phase of the testing.

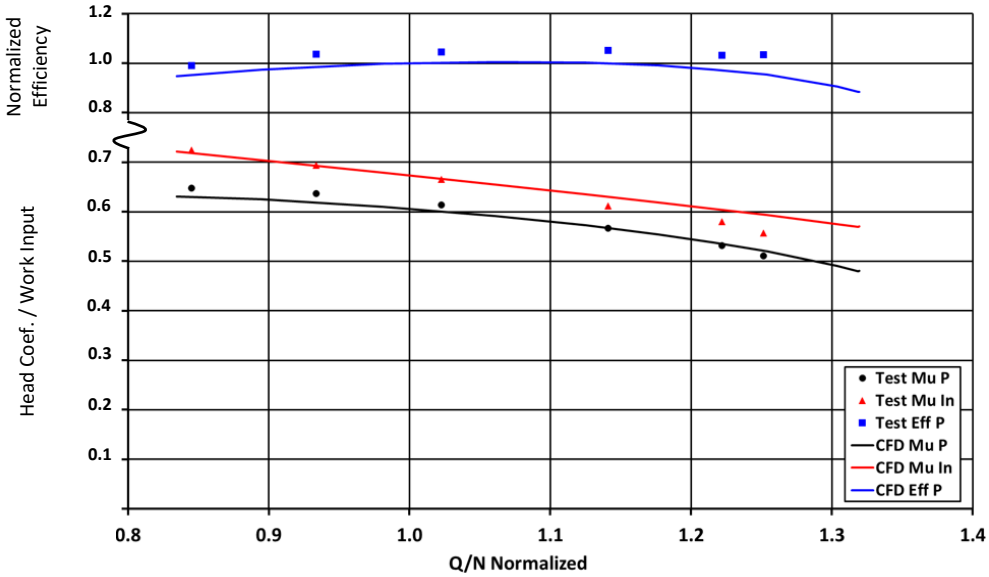

Figure 13 – CFD prediction (solid lines) versus test data (symbols)

CYCLE TIME AND COST CONSIDERATIONS

The experiences with the initial comparison testing and the subsequent test programs on the new stage provided valuable data on the cycle time and cost reductions achievable via the use of polymer components. Of greatest significance was the reduction in time required to acquire the impeller. The average time required to obtain a metallic impeller (aluminum or steel) ranged from eight to twelve weeks while the polymer impellers were built in one to two weeks, achieving a cycle time reduction of at least 75%. Further, the cost of the polymer impeller was 40% (or less) of the metal impeller cost for the size typically used in the test vehicle. Similar cost and cycle time reductions were realized for the associated stationary components. The result was a significant reduction in the cost and cycle time for assembling the aero flow path for a new compressor stage. It was now possible to build and test a completely new stage design in roughly a month and a half as opposed to the two to three months using standard metal components.

Beyond the cost and cycle time savings attributed to component fabrication, there were other advantages related to the use of polymer components. Given the lighter weight of the non-metallic parts, they were much easier to handle, thereby reducing the effort to assemble the builds. In many situations, assembly no longer required cranes or the like to install the parts into the rig. Further, the reduced weight of the impeller reduced rotordynamic concerns during testing. Finally, if geometric changes were needed, it was possible to very quickly print a new or replacement part, install it in the rig and be ready to continue the test program.

Finally, it is important to consider the reduction in "time to market" that can be achieved through the use of polymer test components; that is, the time it takes to develop, test and release new component or product designs to the marketplace. Reducing the "time to market" is advantageous to both OEMs and end users. OEMs reap benefits by being able to more rapidly release new and improved products to clients and by more quickly acquiring validation data to demonstrate the value of the new designs to clients. End users also benefit from the reduced "time to market" because they can more quickly incorporate these new designs or products into their systems, thereby improving production and/or reducing operating costs.

LOOKING FORWARD

Though significant knowledge and experience were gleaned in the execution of this project, the team also recognized that further advances and/or improvements can be made in the construction of non-metallic components. One enhancement is to develop an additive manufacturing method (or printing scheme) that eliminates or significantly reduces the anisotropic material conditions. For example, it might be possible to deposit the material in a circular or circumferential pattern to achieve more uniform properties in the "X-Y" direction (referencing Figure 5). It might eventually be possible to deposit material in sheets rather than beads in the size necessary for test rig components, again improving "X-Y" uniformity. More uniform "X-Y" material properties would reduce concerns regarding non-axisymmetric deflections in the rotating components. Development of more robust non-metallic materials that would allow even higher rotational speeds, temperatures and/or pressures would also be beneficial. Printing techniques that yield smoother surface finishes with the need for post-print finishing would also be advantageous.

Further research is also needed into different styles of impellers. The impellers tested during this investigation were covered (or shrouded) and contained full-inducer or partial inducer blading. Further experience is needed in testing non-inducer style impellers and open impellers constructed from non-metallic materials.

Though there remain lessons to be learned and hurdles to overcome in the wider spread application of polymers in turbomachinery, the progress made to date has clearly demonstrated the long-term potential for non-metallic components in realizing more rapid product development and validation. As confidence grows in the use of polymers for development testing, it will be possible to justify the cost of acquiring the necessary additive manufacturing equipment for use at the OEM facility.

CONCLUDING REMARKS

The advances in additive manufacturing or 3-D printing of non-metallic materials has provided centrifugal compressor OEMs with an opportunity to reduce the cycle time and costs associated with development and validation of new components and products. Polymers have been developed that can withstand the stress levels necessary to aerodynamically testing both stationary and rotating compressor components. The paper traces the development efforts that the OEM undertook to gain the knowledge and experience necessary to safely use non-metallic components in their test vehicle. Knowledge was also gained on the strengths, idiosyncrasies and limitations of the current printing techniques and non-metallic materials. The effort also increased confidence in using polymer components for performance validation testing as comparative testing of polymer and metal impellers agreed quite well.

Finally, non-metallic labyrinth seals have been in use for many years. At some point in the not-too-distant future, advances in materials and additive manufacturing methods will reach a point that the industry will use non-metallic primary flow path components, including impellers, in field installations. For now, the benefits will be derived via rapid prototyping of new components and products to more swiftly deliver these cost and energy-saving concepts to the marketplace.

NOMENCLATURE

A0 = gas sonic velocity
D = Impeller diameter in inches
FEA = Finite element analysis
Mu In = Work input
Mu P = Polytropic head coefficient
N = rotational speed in rpm
Q = volumetric flow in actual cubic feet per minute
rpm = rotations per minute
U2 = impeller tip speed in feet/second
ϕ = flow coefficient = $700.33\ Q/ND^3$
μin = surface finish in micro-inches

ACKNOWLEDGEMENTS

The authors thank co-workers Chuck Dunn, Jenny Quan, Mike Smith, Andrew Ranz and Ed Kunkel for their help during the execution of this project. We also thank Siemens Energy for funding the study and supporting publication of this document. Finally, we thank the Texas A&M Turbomachinery Lab for organizing the Turbo/Pump Symposium and providing an excellent venue to publish this paper.

REFERENCES

Bianchini, A., Carnevale, E., Biliotti, D., Altamore, M., Cangemi, E., Giachi, M., Rubino, D., Tapinassi, L., Ferrara, G., Ferrari, L., 2015, "Development of a research rig for advanced analyses in centrifugal compressors," 70th Conference of the ATI Engineering Association.

Guidotti, E., Tapinassi, L., Toni, L., Bianchi, L., Gaetani, P., and Persico, G., 2011, "Experimental and Numerical Analysis of the Flow Field in the impeller of a Centrifugal Compressor Stage at a Design point", ASME paper no. GT2011-45036.

Killi, S. and Morrison, A., 2016, "FEA and 3D Printing, The Perfect Match?" International Journal of Mechanical Systems Engineering, Volume 2.

Kim, G. D. and Oh, Y. T., 2008, "A benchmark study on rapid prototyping processes and machines: quantitative comparisons of mechanical properties, accuracy, roughness, speed, and material cost," Proceedings of the Institution of Mechanical Engineers, vol. 222, no. 2, pp. 201–215.

Schmitt, M., and Kim, I.Y., 2019, "Experimental Infill Testing and Optimization for FDM Additive Manufacturing", SMSD Lab at Queen's University (*presentation*).

Sorokes, J.M. and Welch, J.P., 1991, "Centrifugal Compressor Performance Enhancement Though the Use of a Single Stage Development Rig," Turbomachinery Symposium Proceedings, Texas A&M, pp 101-112.

Sorokes, J.M. and Koch, J.M., 1996, "The Use of Single and Multi-Stage Test Vehicles in the Development of the Dresser-Rand DATUM Compressor," Dresser-Rand Technology Journal.

Sorokes, J., Kuzdzal, M., Peer, D., Lupkes, K., Saretto, S., Srinivasan, R., 2017, "Design and Testing of a High-Pressure-Ratio Centrifugal Stage – Probing the Aerodynamic & Mechanical Limits," Turbomachinery Symposium Proceedings, Texas A&M, 2017

T. Wohlers, 2011, "Making products by using additive manufacturing," Manufacturing Engineering, vol. 146, no. 4, pp. 70–74.

Wong, K. and Hernandez, A., 2012, "A Review of Additive Manufacturing," ISRN Mechanical Engineering, Volume 2012, Article ID 208760.